Resource

Cell Reports

Rapid Changes in the Translatome during the Conversion of Growth Cones to Synaptic Terminals

Graphical Abstract

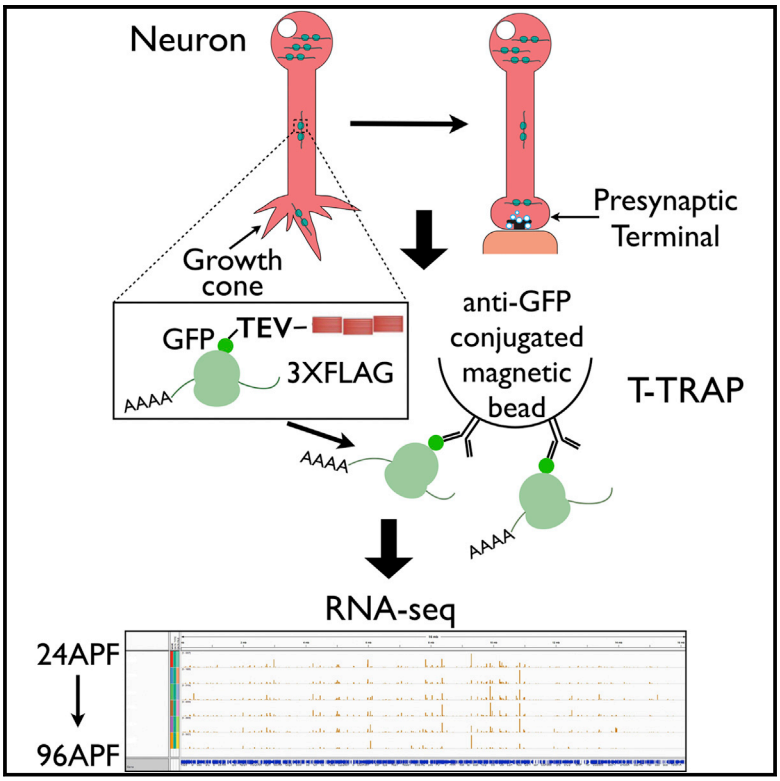

Authors

Kelvin Xi Zhang, Liming Tan, Matteo Pellegrini, S. Lawrence Zipursky, Jason M. McEwen

Correspondence

lzipursky@mednet.ucla.edu

In Brief

Using a tandemly tagged ribosome trap (T-TRAP) and RNA sequencing (RNA-seq), Zhang et al. take advantage of the synchronous conversion of *Drosophila* photoreceptor growth cones into presynaptic terminals to explore global changes in gene expression associated with this step in neuronal differentiation.

Highlights

- Tandemly tagged ribosome affinity purification of RNA from neuronal cell types
- Changes in mRNA associated with ribosomes during presynaptic differentiation
- Dramatic changes in cell surface protein expression with presynaptic differentiation
- Changes in 3′ UTRs in mRNAs for presynaptic proteins during development

Zhang et al., 2016, Cell Reports *14*, 1258–1271
February 9, 2016
http://dx.doi.org/10.1016/j.celrep.2015.12.102

OPEN ACCESS
CellPress

Cell Reports
Resource

Rapid Changes in the Translatome during the Conversion of Growth Cones to Synaptic Terminals

Kelvin Xi Zhang,[1] Liming Tan,[1] Matteo Pellegrini,[2] S. Lawrence Zipursky,[1,*] and Jason M. McEwen[1]
[1]Department of Biological Chemistry, Howard Hughes Medical Institute, David Geffen School of Medicine, University of California, Los Angeles, Los Angeles CA 90095, USA
[2]Department of Molecular, Cell and Developmental Biology, University of California Los Angeles, P.O. Box 951606, Los Angeles, CA 90095, USA
*Correspondence: lzipursky@mednet.ucla.edu
http://dx.doi.org/10.1016/j.celrep.2015.12.102

SUMMARY

A common step in the formation of neural circuits is the conversion of growth cones to presynaptic terminals. Characterizing patterns of global gene expression during this process is problematic due to the cellular diversity of the brain and the complex temporal dynamics of development. Here, we take advantage of the synchronous conversion of *Drosophila* photoreceptor growth cones into presynaptic terminals to explore global changes in gene expression during presynaptic differentiation. Using a tandemly tagged ribosome trap (T-TRAP) and RNA sequencing (RNA-seq) at multiple developmental times, we observed dramatic changes in coding and non-coding RNAs with presynaptic differentiation. Marked changes in the mRNA encoding transmembrane and secreted proteins occurred preferentially. The 3′ UTRs of transcripts encoding synaptic proteins were preferentially lengthened, and these extended UTRs were preferentially enriched for sites recognized by RNA binding proteins. These data provide a rich resource for uncovering the regulatory logic underlying presynaptic differentiation.

INTRODUCTION

Uncovering the genetic programs regulating neural development remains a central problem in neuroscience. Genetic screens have uncovered genes regulating specific steps in neural circuit formation, including cell fate determination, axon guidance, and synapse formation (Desai et al., 1988; Newsome et al., 2000; Zallen et al., 1999; Kidd et al., 1998). Biochemical and molecular biological approaches have also led to the identification of specific genes and the proteins they encode which regulate distinct steps in circuit assembly (Serafini et al., 1994; Cheng et al., 1995; Schmucker et al., 2000). These single gene approaches have been highly effective in dissecting the genetic programs regulating specific steps in neural development.

Recent advances in high-throughput RNA sequencing (RNA-seq) technologies provide an opportunity to assess the global patterns of gene expression during neural development and to relate these to specific genetic programs. In principle, global studies would be most informative in systems where traditional genetic approaches could be applied to establish causal relationships alluded to from correlations discovered in global studies. *Drosophila* offers numerous advantages for combining these approaches. Many cell-type-specific markers enable isolation of mRNA from specific neurons and a palette of genetic approaches allow for incisive phenotypic analyses (Nern et al., 2015; Venken et al., 2011). The fly visual system is particularly well-suited to high-throughput sequencing approaches, as there are numerous different neuronal cell types, and many of these are present in relatively large numbers (Tuthill et al., 2013).

The fly visual system comprises the retina or compound eye that detects light and the optic lobe or ganglia that process visual information. The eye contains some 750 modules called ommatidia and they, in turn, each comprise eight photoreceptor (R) cells. These include R1–R6 neurons, which form synapses with target neurons in the first optic ganglion, the lamina, and the R7 and R8 neurons with distinct visual pigments and synaptic targets in the second optic ganglion, the medulla. Although early steps in R cell development occur in this asynchronous fashion (Hadjieconomou et al., 2011), the conversion of R cell growth cones to synaptic terminals occurs synchronously (Chen et al., 2014). This provides a unique opportunity to explore changes in gene expression occurring in a global fashion associated with this critical step in neuronal differentiation.

Presynaptic differentiation has been studied through genetic and biochemical approaches. It is a complex process involving multiple steps (Chia et al., 2013). These include the transport of active zone and synaptic vesicle components to the presynaptic terminus and the complex interplay between these and the actin cytoskeleton during the assembly of the presynaptic apparatus. In addition, this must be coordinated with the recognition between appropriate synaptic partners, the assembly of an adhesive synaptic complex between the pre- and postsynaptic membrane and the maintenance through secreted signals at synapses.

Here, we set out to provide a description of the changes in gene expression that occur during presynaptic differentiation

at a global scale. Several different approaches have been described for isolating RNA from neurons for mRNA sequencing studies. These include using fluorescent cell tags for isolating neurons by manual picking after tissue dissociation or through fluorescence-activated cell sorting (FACs) (Abruzzi et al., 2015). The INTACT technique utilizes cell-specific expression of a nuclear envelope tag followed by affinity purification of nuclei (Henry et al., 2012; Steiner et al., 2012). The tagged ribosomal affinity purification (TRAP) technique utilizes affinity purification of ribosomes associated with mRNA from lysates prepared from tissues where an epitope-tagged ribosomal protein is selectively expressed in neurons of interest (Doyle et al., 2008; Heiman et al., 2008). Each of these techniques leads to the isolation of a specific pool of mRNA and has provided effective ways of characterizing expression of genes in specific cell types.

As we were particularly interested in understanding the interactions of developing growth cones with their environment and, hence, the proteome rather than the transcriptome, we sought a method of mRNA isolation more likely to reflect differences in protein expression than gene expression more generally. We, thus, set out to identify transcripts associated with ribosomes in R cells using a modified version of the TRAP technique, called tandemly(T)-TRAP. Here, we incorporated an additional tag for a second round of affinity purification of ribosomes from specific neurons. This two-step purification increased the specificity of mRNA isolation, thereby significantly reducing the noise from non-specific association of transcripts expressed in other cells encountered using TRAP. In this paper, we describe changes in gene expression in R cells during presynaptic differentiation. These studies uncovered prominent and dynamic changes in patterns of expression of cell surface and secreted proteins associated with the transformation of growth cones to synaptic terminals and suggest a selective role for post-transcriptional regulatory mechanisms in regulating presynaptic differentiation.

RESULTS

T-TRAP Purification of mRNA

To assess changes in gene expression associated with the conversion of R cell growth cones to presynaptic terminals, we purified mRNA associated with ribosomes selectively from R cells before, during, and after synapse formation (Figure 1A; see below) and analyzed these via RNA-seq. To increase the signal to noise in the TRAP method (Doyle et al., 2008; Heiman et al., 2008), we included a second tag to facilitate a second affinity purification step. We refer to this method as T-TRAP (see below and Experimental Procedures). We modified the N terminus of the *Drosophila* ribosomal protein RpL10 with two tandemly arranged epitopes, 3X FLAG and GFP, separated by the Tobacco Etch Virus (TEV) protease site and expressed this in specific cell types using the GAL4/upstream activating system (UAS) (Figure 1B). In brief, ribosomes from extracts prepared in the presence of cycloheximide were immunoprecipitated with anti-FLAG antibody containing beads, followed by cleavage with TEV protease to release the ribosome from the beads. Ribosomes were then immunoprecipitated again with antibodies to GFP, mRNA was extracted, and RNA-seq libraries were prepared (see Experimental Procedures).

To profile R cell mRNA, we used *chaoptic-Gal4* (*chp-Gal4*) to selectively drive the modified RpL10 protein under UAS control in these cells. The tagged ribosomal protein was seen in the cell bodies and, at lower levels, in axon terminals of R cells (Figure 1C). No evidence of toxicity was observed at the level of light microscopy; R cell morphology was indistinguishable from wild-type as assessed at multiple stages of development and in the adult. In addition, defects were not observed in animals in which the tag was expressed ubiquitously during development. Quantitative western blots revealed that the level of tagged Rpl10 protein normalized to the number of R cells remained constant between 40 and 65 hr; the levels at 24 and 35 hr were 33% and 160% to that observed at 40 hr. As normalized transcript levels were compared these differences do not affect comparisons of reads per kilobase of a specific mRNA per million reads (RPKM) values between samples.

To assess purification, we used qPCR to compare the enrichment of known R cell-specific genes (e.g., [*chp*] and *senseless*) to genes expressed in the optic lobe that are not expressed in R cells (e.g., *apterous*, *brain-specific homeobox*, and *single-minded*). Levels of two retina-specific and three optic lobe-specific transcripts were assessed in extracts prepared from dissected tissues including both the optic lobe and retina at 24 hr after pupae formation (APF) and compared to the levels in the complexes prepared by TRAP and T-TRAP. The levels were normalized to the ribosomal protein RpL11 in extracts and in the immunoprecipitants. For TRAP, the enrichment of retinal-specific genes over optic lobe genes was between one to ten times (Figures 1D and S2). By contrast, for T-TRAP the enrichment through the two-step purification was 25–500 times (see Experimental Procedures for calculations). This increase in enrichment is attributed to a significant depletion of optic lobe transcripts. As expected, this increase in specificity through the second round of immunoprecipitation comes at a cost of decreased yield of mRNA (~30% compared to TRAP).

cDNA libraries were prepared from mRNA associated with the affinity purified ribosomes and sequenced using an Illumina HiSeq 2000 (Figures 1E and S1; Experimental Procedures). As libraries were generated by first strand synthesis using oligo dT, there was a 3′-bias in the sequences obtained. The correlation in the distribution of RPKM values between biological replicates for each time point was excellent with an average Pearson's r of 0.99 (Figures 2A and 2B). By contrast, the further time points were away from each other, the lower the correlation score (i.e., from 0.97 to 0.77). Importantly, the correlation of RNA-seq data between biological replicates using T-TRAP was considerably improved over TRAP (0.99 versus 0.93) (Figures 2A and 2B; see Experimental Procedures for details). This is consistent with the additional affinity purification step resulting in an increase in signal-to-noise. We performed a principal component analysis on R cell expression profiles and found seven distinct subpopulations during R cell development, clearly distinguishable by the first principal component (PC1, 38% of the total variation; Figure 2C). We restricted our analysis to genes with RPKM values >1 at one or more time points (see Experimental Procedures). A total of 9,806 genes fell into this category. This

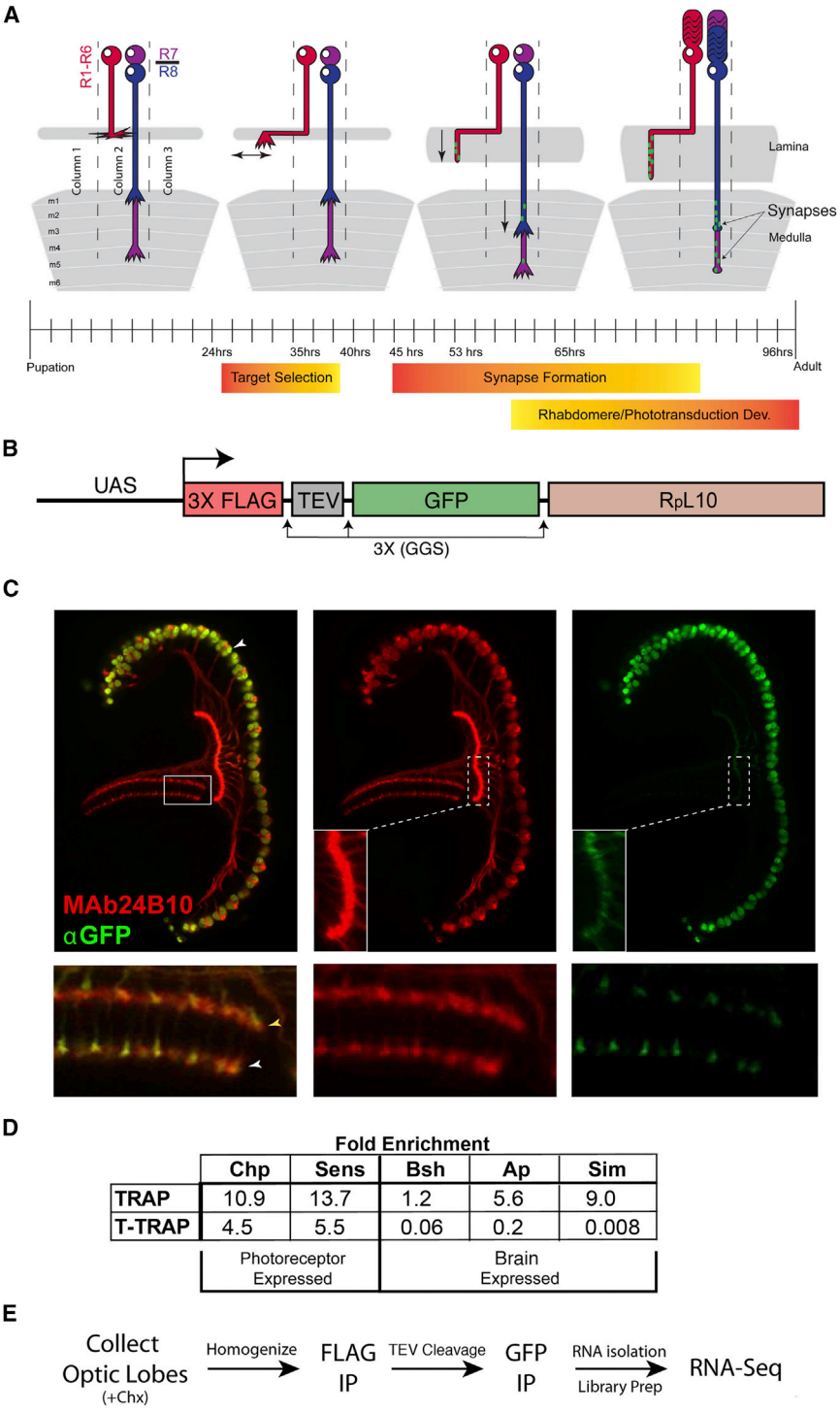

Figure 1. T-TRAP Method for RNA-Seq from Developing R Cells

(A) Schematic of R cell differentiation during pupal development. Target selection period refers to R1–R6. Target selection for R7 and R8 overlaps with the early phase of synapse formation (i.e., post 45 hr).

(B) Schematic of the tandem-tagged ribosomal affinity purification (T-TRAP) construct. The N terminus of the *Drosophila* ribosomal protein L10 (RpL10) coding region was fused to two tandemly arranged epitopes (3xFLAG and GFP) separated by the TEV protease site. 3x (GS) refers to three tandemly arrayed tripeptide sequences (glycine, glycine, serine) used as linker segments.

(C) Tagged RpL10 was selectively expressed in R cells using Gal4 driven by a Chp enhancer element. Upper panels show low magnification, 63x images of eye and part of the optic lobes (i.e., the lamina and medulla comprising synaptic targets for R cell axons) at 24 hr APF. Tagged RpL10 protein accumulates in R cell bodies (white arrowhead), and in the growth cones of R1–R6 (insets), and R7 and R8 (lower panels: R7, yellow arrowhead; R8, white arrowhead). The tagged RpL10 was visualized with an antibody to GFP and R cells were visualized with MAb24B10.

(D) qPCR from RNA isolated from R cells using TRAP and T-TRAP. The TRAP construct comprises from the N terminus, GFP followed by RpL10. Enrichment represents the fold increase between the level of the mRNA indicated and an mRNA encoding a ribosomal subunit RpL11 (see text).

(E) Summary of T-TRAP RNA-seq. Chx, cycloheximide.

See also Figures S1 and S2.

represents 66.3% of the 14,794 genes encoding proteins annotated in *Drosophila*. In addition to mRNA encoding proteins, the expression of 578 long intergenic non-coding RNAs (lincRNAs) were also observed with RPKM values >1 at one or more time points. We describe the analysis of lincRNAs in the Supplementary Information and in Figure S3 and Table S3.

Dynamic Changes in Gene Expression during Conversion of Growth Cones to Presynaptic Terminals

Although early R cell development is asynchronous, from 24 APF onward the development of R cell terminals occurs in a largely synchronous fashion. We chose seven time points for RNA-seq analysis of R cells during pupal development corresponding to 24, 35, 40, 45, 53, 65, and 96 hr APF. These time intervals correlate with specific steps in R cell development (see Figure 1A):

1. 24–35 hr APF: R1–R6 growth cones undergo a rearrangement within the lamina plexus (Clandinin and Zipursky, 2000; Lee et al., 2003; Bate, 1993). No changes are seen in the growth cones of R7 and R8.
2. 35–40 hr APF: growth cones do not alter their positions or their morphologies.

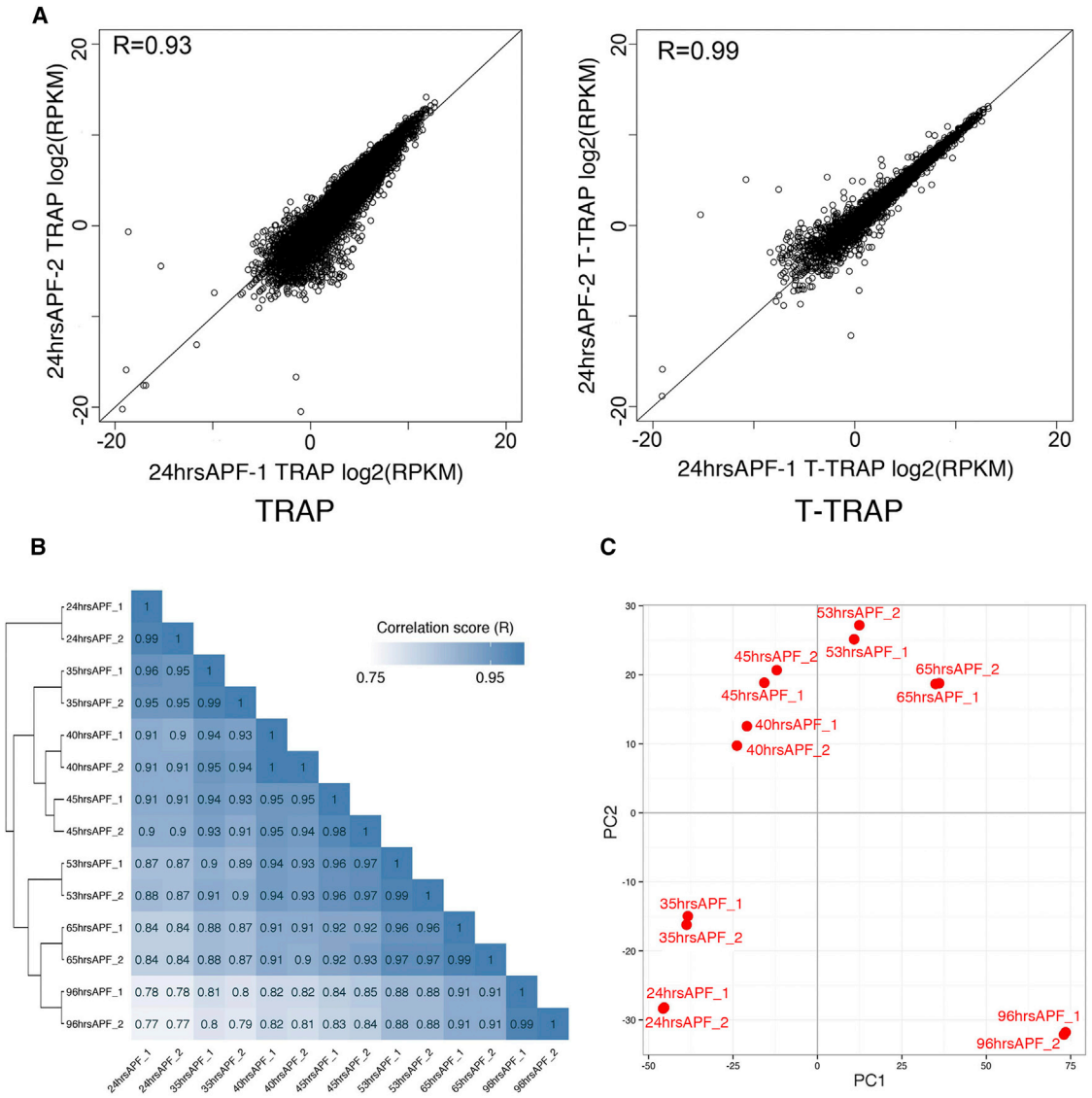

Figure 2. Correlation of RNA-Seq Data from Different Libraries

(A) Scatterplot comparison of biological replicates using the single purification approach (TRAP) and the double purification approach (T-TRAP).

(B) Correlograms showing the correlation score matrix across all libraries at all time points.

(C) Principal component analysis (PCA) of expression in R cells for seven time points. PC1, first principle component; PC2, second principle component. R, Pearson correlation coefficient.

3. 40–45 hr APF: this interval marks the onset of the morphological transformation of R cell growth cones of each class into presynaptic terminals (Chen et al., 2014).
4. 45–53 hr APF: conversion of bulbous growth cones to elongated shape of synaptic terminals is complete. Bruchpilot (Brp) puncta, markers for the presynaptic active zone, begin to accumulate (Chen et al., 2014).
5. Post 53 hr APF: postsynaptic differentiation in target neurons occurs (Chen et al., 2014). Maturation of synaptic terminals overlaps with the development of the rhabdomere, the photosensitive organelle containing rhodopsin (Kumar and Ready, 1995).

In summary, the conversion of R cell growth cones to differentiating presynaptic structures takes place between 35 and 53 hr APF, spanning four time points in our time series.

We sought to assess how many genes exhibited marked changes in their levels of expression between different time points (Figure 3). Here, we performed the differential expression analysis between two successive time points with an adjusted p value < 0.001 and plotted the number of genes, with RPKM values >1 at any given time point, that changed five times or more (Figure 3A). As expected, there is a substantial change during the 30 hr time interval between 65–96 hr APF corresponding to the massive change in morphology and the acquisition of

phototransduction properties in these cells. Importantly, changes in the expression of many genes were seen in two narrow time intervals (i.e., 5 hr, 35–40 hr, and 40–45 hr), corresponding to a period prior to and during the onset of presynaptic differentiation, respectively. Between 35–40 hr APF, just before the onset of presynaptic differentiation, ~450 genes were up or downregulated by greater than five times with more genes downregulated during this interval. A similar number of genes were regulated by greater than five times between 40–45 hr, corresponding to the onset of presynaptic differentiation. By contrast, considerably more genes were upregulated than downregulated during this second interval. Interestingly, the changes during the subsequent two intervals (45–53 hr APF and 53–65 hr APF) were less pronounced. The rate of addition of presynaptic active zones in all three classes of photoreceptor neurons during this period occurs in a largely linear fashion (Chen et al., 2014). Thus, marked changes in gene expression were seen just prior to synapse formation (i.e., 35–40 hr APF) and coincident with the onset of the conversion of a growth cone to a synaptic terminal (i.e., 40–45 hr).

Changes in mRNA Encoding Cell Surface and Secreted Proteins Associated with Ribosomes during Conversion of Growth Cones to Presynaptic Terminals

To obtain a global view of the biological processes represented in these differentially expressed genes, we carried out Gene Ontology (GO) term enrichment analysis using a p value of 0.05 (Figure 3B). There was an increase in genes expressed during later stages (from 65–96 hr APF) involved in photosensitivity and neuronal function, consistent with the terminal differentiation of these cells into photoreceptor neurons. In addition, a marked change in gene expression was observed between 40–45 hr APF coincident with the onset of presynaptic differentiation. GO enrichment analysis revealed preferential increases in the expression of genes during this interval involved in "cell surface receptor-linked signal transduction," "cell adhesion," "extracellular structure organization," "regulation of membrane potential," "ion transport," and "neurological system process." The marked changes in chitin metabolism seen in this time interval were also observed in T-TRAP of lamina neurons (data not shown) and thus this is likely to represent background due to high levels of expression associated with the formation of the lens and other chitinous tissues. The enrichment in "cell surface-linked signal transduction" and "cell adhesion" and "extracellular structure organization" are consistent with the cellular processes associated with the transformation of the growth cone to a presynaptic terminal.

Interestingly, in contrast to the increase in "cell surface receptor-linked signal transduction" and "cell adhesion" gene categories observed between 40–45 hr APF, there was a substantial decrease in the levels of this class of transcripts between 35–40 hr APF (see below). This corresponds to a stage in which growth cones largely remain "quiescent," where there are no obvious changes in growth cone dynamics or position. Thus, a marked re-programming of gene expression regulating intercellular communication occurs during two sequential time intervals corresponding to a period following axon guidance and the onset of the conversion of R cell growth cones to presynaptic terminals.

We sought to explore the expression pattern of genes encoding cell surface and secreted proteins in more detail. Examination of GO terms in FlyBase revealed that some proteins with known functions in axon guidance and cell adhesion were not included in the GO terms "cell adhesion" and "cell surface receptor-linked signal transduction." To provide a more comprehensive assessment of the expression patterns, we used the set of 968 genes identified by Kurusu et al. (2008) as putative cell surface and secreted proteins encoded in the fly genome and generated additional "hand" curated lists for an additional 15 categories (Table S1).

We focused on three time intervals marking the transition from growth cones to differentiating presynaptic terminals, including a stage prior to overt changes in growth cone morphology (35–40 hr), the onset of morphological transformation to a presynaptic terminal (40–45 hr), and the appearance of presynaptic active zones (45–53 hr APF), respectively (Figure 3C). Changes in selective expression of cell surface proteins for all three time intervals were observed. Between 35–40 hr APF, 69 transcripts encoding cell surface/secreted proteins changed by >5-fold. Approximately one-third of these transcripts increased and the remaining two-thirds decreased. By contrast, many more transcripts encoding cell surface proteins increased during the 40–45 hr APF interval, with 62 transcripts changing five times or more, of which 56 increased and the remaining six decreased. In addition, between 35–40 and 45–53 hr APF there were selective changes in genes associated with photoreceptor function, consistent with the role of these cells in the adult. Although genes in other categories, including those encoding synaptic proteins (see below), were differentially expressed, the number of such genes was not different from that expected by chance.

Many of the genes encoding cell surface and secreted proteins that were upregulated between 40–45 hr APF, were downregulated in the developmental window just prior to this interval (i.e., 35–40 hr APF). The transcripts for some 25 cell surface proteins changed during 45–53 hr APF, with ~50% increasing and the remaining decreasing (Figures 3C and 3D). In summary, in the union set of transcripts changing between 40–45, 45–53, and 40–53 hr APF, corresponding to the onset of the final targeting step and onset of presynaptic differentiation, 125 cell surface proteins were up or downregulated by greater than five times.

We categorized the patterns of expression of genes in the union set that go up greater than five times into three major classes (Figures 4A and 4B): class I genes were downregulated before being upregulated between 40–53 hr APF; class II genes were unchanged between 35–40 hr APF and were subsequently upregulated between 40–45 hr APF; and class III genes were upregulated between 45–53 hr APF. These fall into different protein families (Figure 4C; see Table S8 for a complete list of expression of protein families at all time points). It should be noted that the five times cut-off is arbitrary and, indeed, many other cell surface proteins are present at each time point and may change modestly (e.g., 2- to 4-fold) or not at all (see below). Indeed, several genes known to contribute to wiring during these developmental steps are expressed by a change less than five times between different developmental time points within the broader interval from 35–53 hr APF (data not shown). Nevertheless, the changes in expression of many genes corresponding to discrete

A

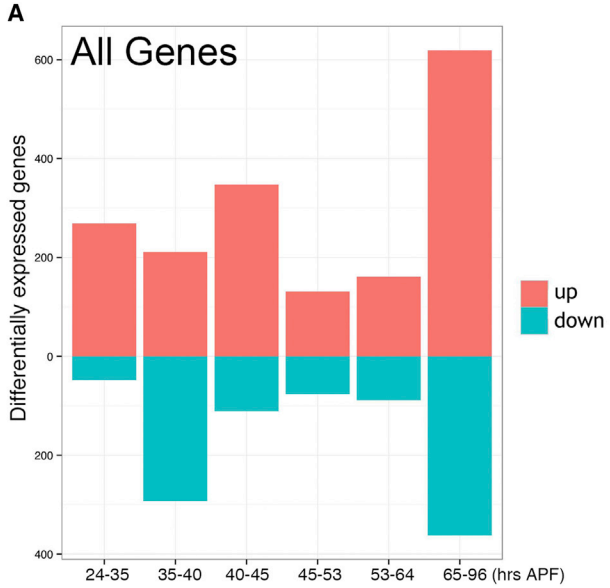

B

C

Biolological category	35-40hrs APF			40-45hrs APF			45-53hrs APF			Total in fly genome
	Up (5X)	Down (5X)	P-value	Up (5X)	Down (5X)	P-value	Up (5X)	Down (5X)	P-value	
cell_surface	21	48	3.00E-07	56	6	1.31E-08	18	12	1.15E-04	950
phototransduction	8	1	1.52E-06	0	1	4.02E-01	10	0	1.40E-09	43
splicing_regulator	1	0	5.18E-02	0	0	9.84E-01	0	0	1.27E-01	150
gap	0	0	1.80E-01	0	0	2.43E-01	0	0	3.06E-01	21
synapse	1	0	3.55E-01	1	1	6.08E-01	0	0	3.25E-01	44
kinase_activity	10	1	4.65E-01	5	2	1.43E-01	0	1	9.64E-01	373
TF	12	12	4.75E-01	15	5	3.35E-01	3	3	9.07E-02	751
actin_binding	1	3	5.25E-01	3	1	6.02E-01	1	0	3.03E-01	120
ecdysone_inducible	1	3	6.66E-01	2	1	4.23E-01	0	2	7.59E-01	109
phosphatase_activity	2	5	7.30E-01	2	4	6.39E-01	1	0	2.00E-01	178
translation_regulation	4	1	8.41E-01	1	3	7.72E-01	0	0	2.63E-01	78
RNA_binding	8	7	9.55E-01	8	11	3.42E-01	0	1	9.98E-01	741
gef	2	1	9.76E-01	1	0	5.82E-01	0	0	3.25E-01	24
membrane_transporter	8	27	9.77E-01	30	3	9.83E-01	4	2	6.55E-02	765
chromatin_assembly	0	0	9.90E-01	1	1	1.63E-01	0	0	9.61E-02	138
microtubule	4	2	9.96E-01	0	1	2.58E-01	0	0	2.16E-01	63

D

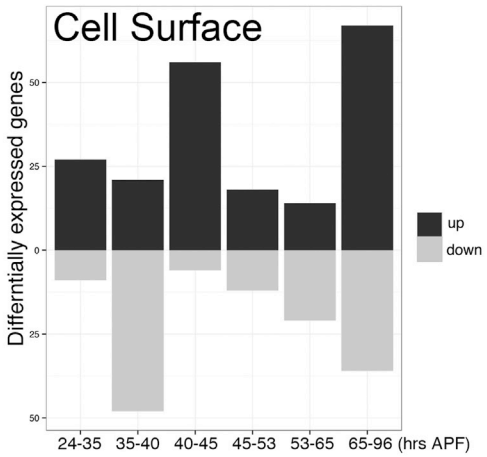

(legend on next page)

development steps in wiring raise the possibility that they play roles at these developmental steps or alternatively that signaling in growth cones changes the spectrum of proteins loaded onto ribosomes for use at later stages.

Comparison between FACS and T-TRAP Generated Transcriptomes

We next sought to assess whether the changes observed in T-TRAP reflected changes in transcription or in post-transcriptional mechanisms (i.e., association of mRNAs with ribosomes). To do this, we compared patterns of gene expression from FACS-sorted cells, using the GFP in the T-TRAP-labeled RpL10 protein as a marker for cell sorting and mRNA isolated from flies of the same genotype using T-TRAP at two time points, 40 hr and 53 hr APF. We then assessed whether changes in gene expression observed between these two time points reflected changes in transcription or in post-transcriptional mechanisms. There were 669 and 308 transcripts that changed by more than five times between these two time points in T-TRAP and FACS, respectively (Table S2). Of the overlap set of 142 genes differentially expressed between these time points in both the T-TRAP and FACS analysis, 138 were regulated in a similar manner in both FACS and T-TRAP. For 531 differentially expressed genes in T-TRAP (79.3%), however, there was either no change in FACS or the change was in the opposite direction. Thus, although changes in gene expression associated with presynaptic differentiation occur at the level of transcription, the changes in ribosome association suggests that post-transcriptional regulatory mechanisms play a prominent role in presynaptic differentiation.

Changes in Presynaptic 3′ UTR Regulation during Synapse Formation

We next sought to assess the relationship between the expression of genes encoding presynaptic proteins and the transformation of R cell growth cones to presynaptic terminals. Despite the abrupt change in morphology correlated with the transition from growth cones to synaptic terminals and the dramatic changes in the expression of cell surface and secreted proteins associated with this transition, a similar change in the expression of presynaptic proteins, as a class, was not observed (Figure 5A; compare to Figure 4A).

Most genes encoding presynaptic proteins were expressed at moderate levels as early as 24 hr APF, well before synapse formation and these generally increased over time (Table S1). Furthermore, as a class, these genes were no more likely to be upregulated than expected by chance (see Figure 3C). Only five genes encoding known presynaptic proteins exhibited substantial changes in levels between 40 and 53 hr APF. Two synaptic vesicle proteins, synapsin (Syn) and synaptogyrin (Syngr), increase seven times and five times, respectively, during this period. Syngr increases another 32 times between 53–96 hr APF, consistent with its requirement for normal synaptic vesicle biogenesis (Stevens et al., 2012). Adult R cells are densely packed with synaptic vesicles and Syngr expression appears linked to this accumulation. Other transcripts encoding proteins involved with synaptic vesicle function, fusion and recycling (i.e., n-synaptobrevin [n-Syb], synaptosomal-associated protein 25 kDa [SNAP-25], and endophilinA [EndoA]) increased modestly between 53–95 hr APF (two to three times) (Bhattacharya et al., 2002; Guichet et al., 2002; Vilinsky et al., 2002). Transcripts encoding active zone proteins Cacophony (Cac), Straight-jacket (Stj), and Brp increased two to seven times between 24 and 53 hr; the patterns of expression exhibited different kinetics and the level of these transcripts generally decreased by two to ten times by 96 hr APF (Ly et al., 2008; Smith et al., 1996). The level of *highwire* (*hiw*) mRNA, encoding a ubiquitin E3 ligase that acts as a negative regulator of active zones (Wan et al., 2000), was very low at all times points with only one RPKM value >1 at 40 hr APF. Together, these observations are consistent with a role for post-transcriptional regulation during presynaptic differentiation.

Given the implication of the importance of post-transcriptional regulation during synapse formation, we examined the 3′ UTRs of mRNAs encoding presynaptic proteins. We observed that 3′ UTRs of 55% of these genes (45 genes analyzed) changed between 24–96 hr APF (Figure 5; Table S4). By contrast, only 26% of five randomly selected sets of genes (45 genes in each set) during this time period showed changes in their 3′ UTRs. This difference is highly significant ($p = 1.71e-07$, z test). In other systems, enzymes regulating 3′ UTR cleavage and polyadenylation site selection are downregulated during development (Di Giammartino et al., 2011; Ji et al., 2009), thereby resulting in longer 3′ UTRs. Consistent with this, we observed a universal downregulation of enzymes regulating the 3′ UTRs during development. These included the cleavage and polyadenylation specificity factor (CPSF), cleavage stimulation factor (CSTF), and cleavage factor IM (CFIM) ranging from 3.5 times to 44 times from 24–96 hr APF (Table S5). In addition, regulatory factors of the Elav family of RNA binding proteins including Elav, Rpb9, and Fne show dynamic changes in expression (Samson and Chalvet, 2003) (Table S5). Elav protein has been shown to promote the formation of longer 3′ UTRs in the developing fly embryonic nervous system (Hilgers et al., 2012). In developing R cells,

Figure 3. Differential Gene Expression during R Cell Development

(A) The number of upregulated and downregulated genes during R cell development. RPKM values are greater than one (see text).

(B) Enriched biological processes across different stages during R cell development using GO term enrichment analysis. The differentially expressed genes were classified into two categories: upregulated (red) and downregulated (blue).

(C) Biological categories (see text) of differentially regulated genes (five times upregulated and five times downregulated) between 35–40 hr APF, 40–45 hr APF, and 45–53 hr APF. The p value represents the likelihood that the number of genes expressed greater than five times between the indicated time points is significantly different from that expected from a random distribution in each biological category (see Experimental Procedures).

(D) The number cell surface and secreted molecules upregulated and downregulated greater than five times. For both (C) and (D), RPKM for a transcript at one time point must be greater than one and levels between time points are greater than five times.

See also Tables S1 and S2.

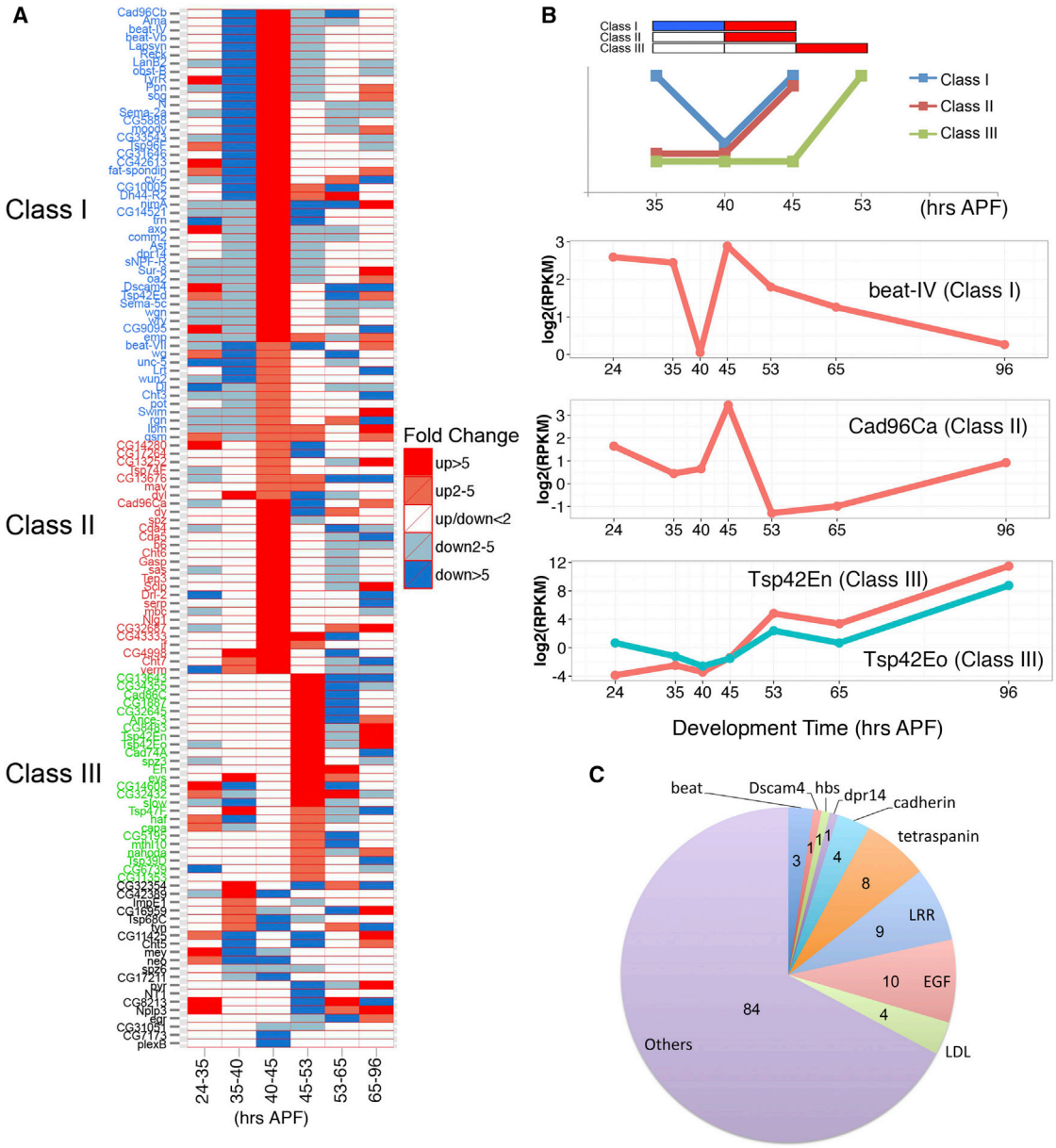

Figure 4. Dynamic Regulation of Cell Surface and Secreted Molecules Expressed during Presynaptic Differentiation

(A) Heatmap showing differential regulation of 125 cell surface or secreted molecules changing greater than 5 times in the union set of differentially expressed genes between 40–45 hr APF, 45–53 hr APF, and 40–53 hr APF. Color code as indicated. Expression for each of transcript is shown across the entire time series. The fold change refers to the significant change in level between two neighboring time points. Note that these are relative changes not absolute values and boxes showing genes with RPKMs less than one in both time points are labeled as "no change" (white).

(B) Schematic presentation of gene expression patterns of a group of genes as indicated. Gene expression patterns of four cell surface or secreted molecules are shown (see text).

(C) Pie chart showing the numbers of 125 differentially expressed genes in different gene families during presynaptic development. There are six Ig superfamily proteins: three Beat paralogs, Dscam4, Hbs, and Dpr14.

See also Table S8.

elav mRNA expression peaks at 40 hr APF and gradually falls to low levels at 96 hr APF. By contrast, Rpb9 increases continuously to high levels at 96 hr APF and Fne shows a complex pattern of regulation with peak levels at both 35 and 45 hr APF before decreasing gradually to low levels by 96 hr APF. Thus, although there is a general trend toward lengthening the 3′ UTR in all genes in R cells as development proceeds, there is a selective increase in 3′ UTR length for genes encoding presynaptic components and correlated changes in mRNAs encoding proteins and paralogs of them, which regulate processing of 3′ UTRs.

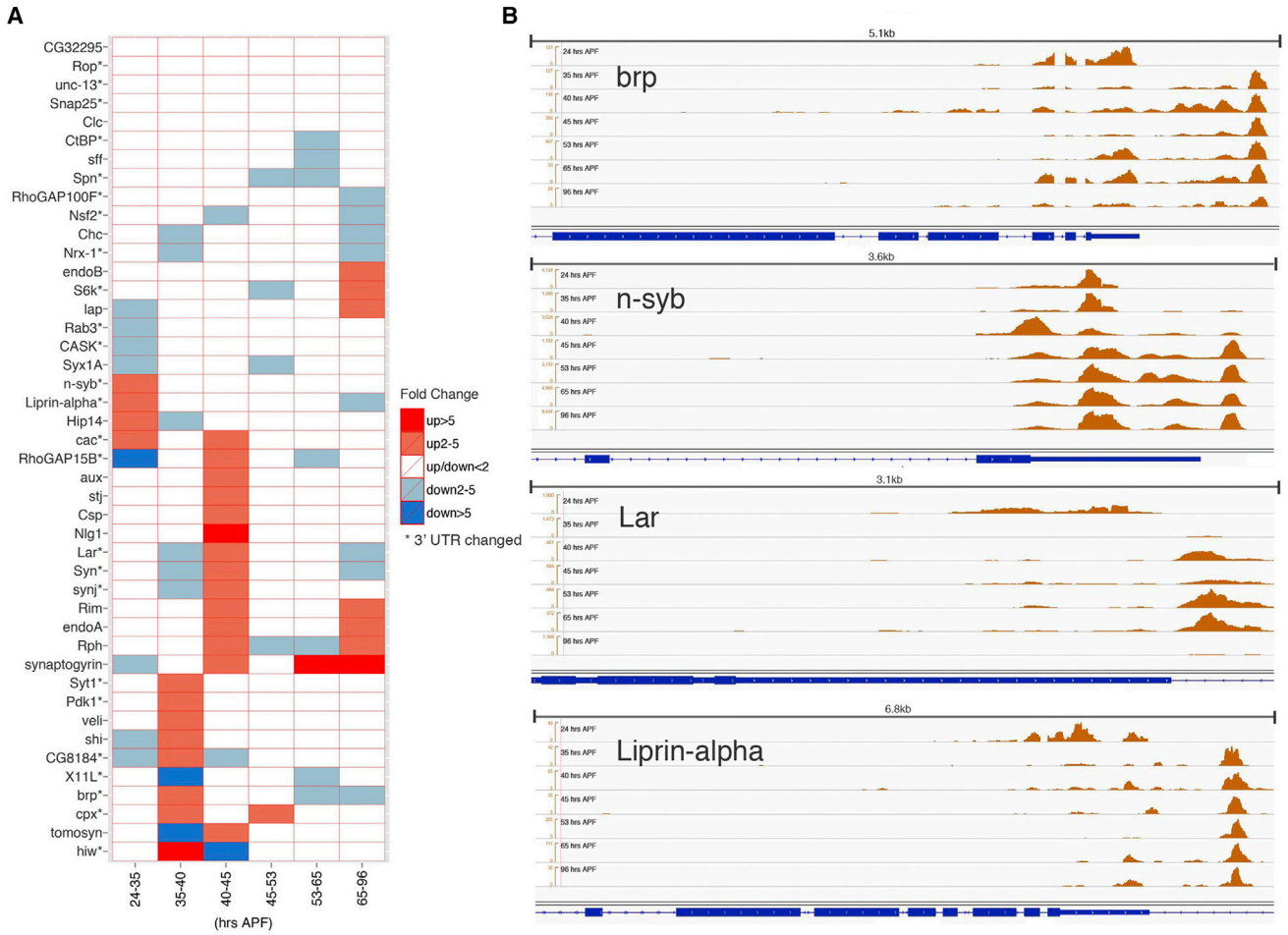

Figure 5. Identification of Alternative 3′ UTRs in Presynaptic Proteins

(A) The heatmap showing gene expression level changes of 45 presynaptic proteins between two adjacent time points during development.

(B) Four examples of transcripts (*brp*, *n-syb*, *Lar*, and *Liprin-alpha*) demonstrating the extended 3′ UTRs during development.

See also Table S6.

Identification of Enriched RNA Binding Proteins Binding Motifs in Synaptic Transcripts

The correlation between presynaptic differentiation and changes in the 3′ UTR of many transcripts encoding synaptic proteins raised the possibility that these regions are sites of translational regulation through microRNAs, RNA binding proteins or both. To explore this possibility, we compared the sequences of synaptic transcripts with extended 3′ UTRs, to those lacking the 3′ UTR extension for binding sites for both microRNA and RNA binding proteins. This comparison included 18 transcripts with 3′ UTR extensions, on average 1.3 kb in length, to 20 transcripts that were not extended, with 3′ UTRs with an average length of 1.1 kb (Table S6).

To test for enrichment of microRNA binding sites within 3′ UTRs, we searched for potential binding sites for 466 known fly microRNAs in the miRBase database (Kozomara and Griffiths-Jones, 2014). The numbers of predicted binding sites found in both classes of 3′ UTRs were very similar ($R = 0.84$, p value < 2.2e-16, Pearson correlation coefficient). This suggests that the transcripts with extended 3′ UTRs in R cells are no more likely to be regulated by microRNAs than their unextended counterparts. Furthermore, the 3′ UTRs were no more likely to contain miRNA binding sites than randomly selected 3′ UTRs (p value = 0.057, z test). Thus, our analysis does not support the notion that the increased length of transcripts reflects an increased propensity of transcripts encoding presynaptic proteins to be regulated by miRNAs.

We next assessed whether extended 3′ UTRs are more likely to be sites of regulation through RNA binding proteins than their counterparts that were not extended. We first performed the RNA binding proteins (RBP) binding site prediction analysis using a list of known position weight matrices (PWMs) of 224 fly RNA binding proteins (Ray et al., 2013). This revealed that RNA binding motifs were over-represented in mRNAs encoding synaptic proteins when compared to random sequences of genomic DNA regardless of whether the 3′ UTRs were extended. Furthermore, there were marked differences between the 3′ UTRs. Thirty significant motifs were found in genes encoding synaptic

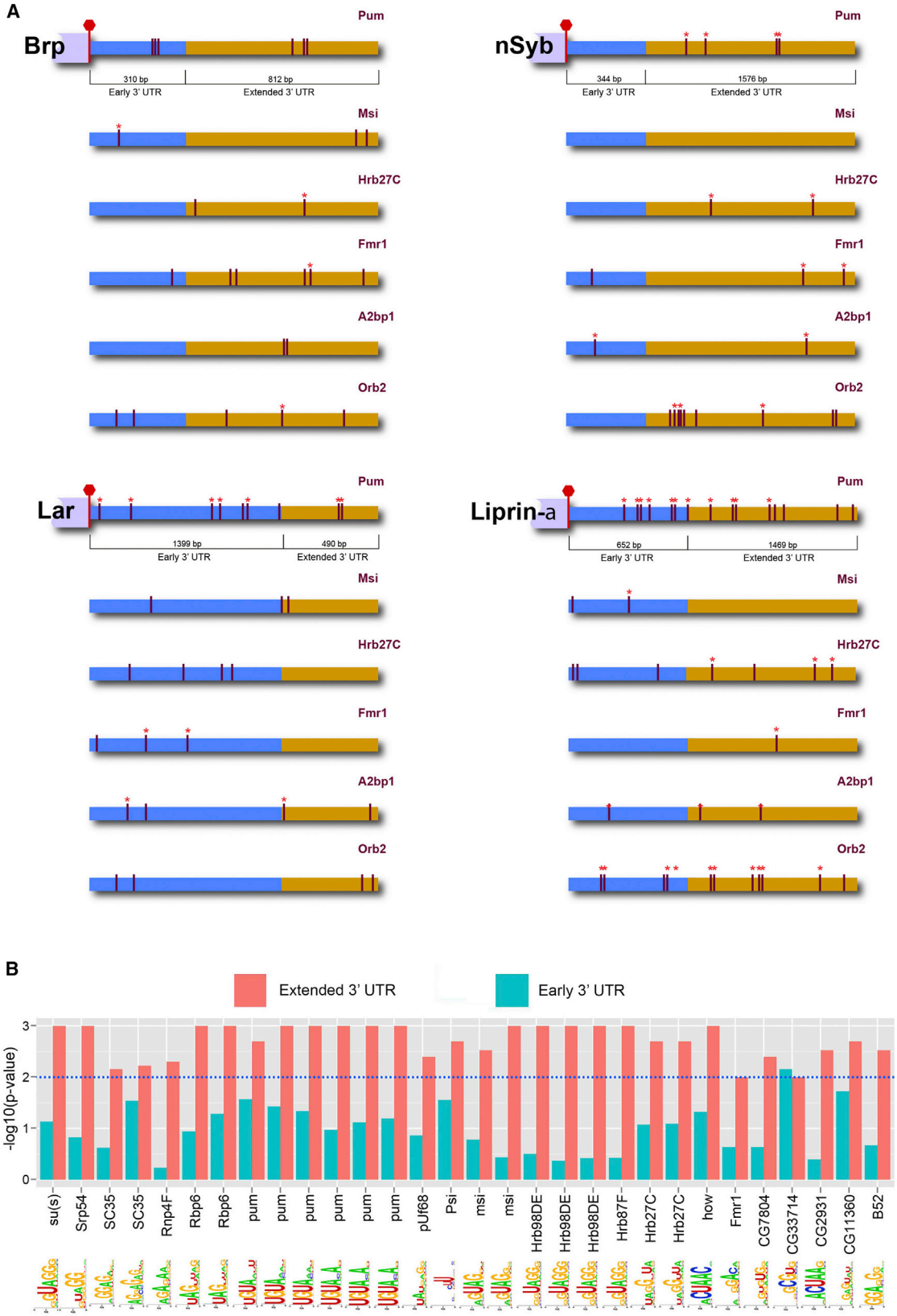

(legend on next page)

proteins with extended 3′ UTR, whereas only one motif was significantly enriched in genes lacking an extended 3′ UTR (i.e., with a p value of 0.01) (Figure 6B). Four examples are shown in Figure 6A. Sequence comparison of all the RBP binding sites between the genomes of 14 insect species revealed that 88.9% (16 out of 18) of the presynaptic genes with extended 3′ UTRs have at least one highly conserved RBP binding site (e.g., asterisks in Figure 6A and Table S7). These findings suggest that post-transcriptional mechanisms contribute significantly to synaptic differentiation.

Interestingly, several RNA binding proteins known to regulate mRNA localization and translation (e.g., 4EHP, Hrb27c, and Imp), were also dynamically regulated during this period. These findings are consistent with the notion that post-transcriptional regulatory mechanisms may play a prominent role in regulating the expression of synaptic components. Several RBPs that exhibited changes in expression during R cell synapse formation and for which binding sites in mRNAs encoding synaptic proteins are enriched have been shown to regulate synaptic strength at the fly neuromuscular junction (Menon et al., 2004) and learning and memory (Keleman et al., 2007). Thus, together these data support the view that post-transcriptional mechanisms play an important role in regulating presynaptic differentiation.

DISCUSSION

Characterization of Gene Expression during Synapse Formation Using T-TRAP

The conversion of a growth cone to a presynaptic terminal is a common step in the neuronal differentiation. As this step occurs synchronously in R cells, these neurons provide a unique opportunity to characterize global patterns of gene expression during this process. We isolated mRNA associated with ribosomes labeled with two tandemly arranged tags (T-TRAP), rather than a single one, separated by a protease recognition site. This facilitated a two-step affinity purification of mRNA associated with ribosomes thereby increasing signal-to-noise and reproducibility between biological replicates over that achieved via TRAP (e.g., from 0.93 to 0.99). This comes at a cost of a significant, though acceptable, decrease in yield (~30%). No developmental or morphological abnormalities resulted from overexpression of the tandem-tagged ribosomal subunit in various cell types, in contrast to overexpression of other tags in the same cells used for mRNA purification, such as the poly A binding protein (J.M.M. and S.L.Z, unpublished data). We have recently modified the transgenes encoding T-TRAP to further reduce background by increasing expression via the inclusion of non-coding sequences enhancing translation (Pfeiffer et al., 2012) and by mitigating the effects of leaky expression of the UAS construct by inserting a transcriptional stop sequences flanked by FRT-recombination sites (unpublished data). Targeting recombinase expression to the cells of interest and coupling this with cell-type-specific expression of GAL4 further increases the cell-type specificity of this method (Golic and Lindquist, 1989). Given the cellular diversity of neural tissue we anticipate that the T-TRAP technique will provide effective ways for isolating transcripts from increasingly smaller subsets of cells in flies and perhaps in mouse as well.

Selective Changes in Transcripts Encoding Cell Surface Proteins with the Onset of Presynaptic Differentiation

The detailed time course of gene expression in R cells during the transformation of R cell growth cones to presynaptic terminals revealed substantial changes in the expression of many mRNAs encoding cell surface proteins, including those implicated in cellular recognition and synapse formation. The changes in expression were highly selective for cell surface and secreted proteins. The only other category with selective expression within this interval was "phototransduction" reflecting a precocious upregulation of a subset of these genes prior to the onset of opsin expression and, hence, photosensitivity. Indeed, just prior to the onset of morphological changes in R cell growth cones preceding their transformation into presynaptic terminals (i.e., 35–40 hr APF), many more mRNAs encoding cell surface components (approximately three times) were downregulated than upregulated. By contrast, during the subsequent time interval correlating with the first morphological manifestation of presynaptic differentiation (i.e., 40–45 hr APF), many more cell surface proteins (approximately ten times) were upregulated than downregulated. The changes in the association of these mRNAs with ribosomes during these time intervals suggests that a massive restructuring of the cell surface plays an important role in the transition of the growth cone to a synaptic terminal. Comparison of expression differences between FACS and T-TRAP indicate that many of these changes occur preferentially at the post-transcriptional level. The complementary and alternating expression of the translational inhibitors, 4EHP and 4E-BP (or Thor) at each time point (i.e., when one is high the other is low), is consistent with expression being highly regulated at the level of translation just prior to and during synapse formation. The changes in the cell surface proteome, however, also reflect the stability of different membrane proteins. As the half-lives of proteins vary over many orders of magnitude, the changes in the ribosome association of mRNAs of proteins encoding different cell surface proteins only represent part of the story. Measuring these changes in axon terminals for proteins in vivo, even for one protein, remains an experimental challenge.

The transcripts changing greater than five times during these intervals included those encoding members of large families of cell surface molecules previously implicated, or shown to be required for, neural circuit formation including immunoglobulin-containing proteins (e.g., Dscam4 and beat-IV) (Fambrough

Figure 6. RNA Binding Proteins Binding Motifs in 3′ UTRs of Presynaptic Proteins

(A) Four transcripts encoding synaptic proteins (*brp*, *n-syb*, *Lar*, and *Liprin-α*) with binding sites for the indicated RNA binding proteins (RBPs) in both early 3′ UTR (blue) and extended 3′ UTR (gold). RBP binding sites highly conserved across species are labeled with asterisks (see text).

(B) Bar plot showing 30 significant RBP binding motifs were found in genes encoding synaptic proteins with extended 3′ UTR (red bar), whereas only one motif was significantly enriched in genes without an extended 3′ UTR (blue bar). The blue dash line indicates a threshold of p value of 0.01.

See also Figure S4 and Tables S6 and S7.

and Goodman, 1996; Millard et al., 2010; Yamagata and Sanes, 2008), leucine-rich repeat containing proteins (e.g., lapsyn) (Guan et al., 2011), cadherins (e.g., Cad96Ca), integrin family members (e.g., *if*), and tetraspanins (Hoang and Chiba, 1998; Kopczynski et al., 1996; Lee et al., 2001). In addition, other proteins that changed considerably during this time, including components of the extracellular matrix (e.g., laminin and various proteases), guidance receptors (e.g., Drl-2), secreted signals (e.g., wingless, semaphorin2a), antagonists of BMP signaling and spatzle family members, regulate various steps in development, including synapse formation, terminal branch morphology, and cell survival (García-Alonso et al., 1996; Liebl et al., 2008; Zhu et al., 2008; Zlatic et al., 2009). These changes are consistent with dynamic intercellular interactions occurring within the neuropil as complex patterns of connections between R cell terminals and their targets are assembled (Rivera-Alba et al., 2011; Takemura et al., 2013).

Post-transcriptional Regulation through 3′ UTRs

Although marked changes in cell surface proteins were readily observed between closely spaced time points prior to and during synapse formation, changes in the levels of transcripts encoding synaptic proteins were modest. A doubling in the length of the 3′ UTRs encoding presynaptic proteins was correlated with an increase in the number of binding sites for RNA binding proteins implicated in regulating mRNA localization, stability and translation. These binding proteins were expressed in R cells, some at constant levels (e.g., Fmr) through the time course examined, whereas others changed considerably (e.g., Hrb27c). Importantly, in each of these extended transcripts at least one RBP binding site is conserved with orthologous transcripts in other *Drosophila* species supporting the notion that these sites are functionally significant. Functional studies in *Caenorhabditis elegans* also support a role for increased 3′ UTR length in regulating presynaptic differentiation, with mutations in a negative regulator of polyadenylation (i.e., favoring shortened 3′ UTR) leading to defects in synapse formation (Van Epps et al., 2010). Together these data suggest that increased 3′ UTR length is an important regulator of presynaptic differentiation and that increased length promotes post-transcriptional regulation through interactions with RNA binding proteins.

Regulation through the 3′ UTRs may also play a more widespread role in regulating presynaptic differentiation (Chia et al., 2014). For instance, actin assembly is required for presynaptic differentiation and actin regulatory proteins are regulated post-transcriptionally via the evolutionarily conserved protein Imp. Imp binds selectively to sequences within the 3′ UTRs of actin regulatory proteins (Medioni et al., 2014). Indeed, biochemical studies in *Drosophila* S2 cells in culture identified 40 actin regulatory proteins with Imp binding sites (Hansen et al., 2015). All of these are expressed in R cells, many at very high levels, during synapse formation. Importantly, in our dataset, Imp transcript is upregulated some 40 times prior to the onset of presynaptic differentiation.

A recent study suggests that different 3′ UTRs may also regulate the transport of membrane proteins to the cell surface (Berkovits and Mayr, 2015). Here, human HuR proteins bind to 3′ UTRs of mRNAs encoding cell surface proteins as they are being translated at the ER. HuR proteins then recruit a protein complex that selectively associates with the C terminus of the nascent polypeptide and this complex, in turn, promotes transport of the newly synthesized protein to the cell surface. There are three *Drosophila* homologs of HuR (Elav, Fne and Rpb9). These three proteins have been implicated in synapse formation in the *Drosophila* neuromuscular junction (Zaharieva et al., 2015), and, as we discussed above, they are also implicated in lengthening of 3′ UTRs. Interestingly, these proteins are expressed in very different and dynamic ways in R cells during synaptic development (Table S5). Rbp9 expression increases continuously between 24 and 53 hr APF with a change of nearly 20 times. By contrast, Elav and Fne are expressed in a largely complementary fashion with peak levels of Elav at 24 and 40 hr APF, whereas Fne shows high levels of expression at 35 and 45 hr APF, with reduced levels at 40 hr APF.

Together, these data suggest that diverse post-transcriptional mechanisms mediated through 3′ UTR sequences play an important role in regulating synapse formation in R cells.

Concluding Remarks

Decades of genetic analysis have provided an extensive tool kit for exploring neural circuit assembly in the fly visual system. Here, progress has been made in large part based on the ability to genetically manipulate specific cell types, single cells, or small subsets of them to assess their phenotypes in an otherwise normal or wild-type background. We recently demonstrated that all R cells progress through synapse formation synchronously. This synchrony within a single fly and the ability to synchronize large numbers of animals at the onset of pupal development, provided a unique opportunity to explore gene expression at a global level during the conversion of growth cones to presynaptic terminals. Coupling this global approach to genetic and functional analysis at the level of single genes provide a unique opportunity to dissect the molecular program underlying synaptic development.

EXPERIMENTAL PROCEDURES

T-TRAP Flies

TRAP and T-TRAP constructs were generated by insertion of dRpL10a with an N-terminal Not-I site following the ATG inserted into pUAST using EcoRI/XbaI. Then a cassette containing either Not-I flanked GFP (TRAP) or Not-I flanked 3xFLAG-TEV-GFP (T-TRAP) was inserted. Flies were injected with either construct and F2 progeny were screened for transgenic animals exhibiting the lowest UAS expression in the absence of GAL4 as assessed by western blot against GFP.

T-TRAP Purification

Brain dissections were performed in dissection buffer (1× HBSS, 2.5 mM HEPES [pH 7.4], 35 mM glucose, 4 mM $NaHCO_3$) containing 100 μg/ml of cycloheximide (CHX). The central brain was discarded and optic lobes and retina were frozen on dry ice and maintained at −80 in Lysis buffer (20 mM HEPES [pH 7.4], 150 mM KCl, 5 mM MgCl + protease inhibitors) containing 100 μg/ml CHX until enough optic lobes were accumulated. For each replicate with the Chp-GAL4 driver, 40 optic lobes were used.

Optic lobes were thawed and homogenized using a motorized Teflon pestle in 500 μl of lysis buffer with RNase inhibitors; one-ninth the volume of Igepal CA-360 was added and the tube is gently inverted, followed by addition of one-ninth the volume of 1,2-diheptanoyl-*sn*-glycero-3-phosphocholine. The tube containing this mixture was inverted and placed on ice for 5 min to lyse

the cells. Lysates were centrifuged at 16,000 rpm for 15 min at 4°C. The supernatant was added to tubes containing anti-FLAG M2 affinity magnetic beads (Sigma) and incubated at 4°C for 1 hr with gentle rotation. Beads were collected and washed three times with Wash Buffer #1 (20 mM HEPES [pH 7.4], 150 mM KCl, 5 mM MgCl, 1% Igepal CA-360) and 500 μl of IP buffer #2 (20 mM HEPES [pH 7.4], 150 mM KCl, 5 mM MgCl, 1% Igepal CA-360, + protease and RNase inhibitors) was added to the beads. Five microliters of TEV protease (10 U/μl) was added (Life Technologies) and in some cases 3 μl Turbo DNase (2 U/μl) (Ambion), and mixtures were incubated at room temperature for 1 hr with gentle rotation. The supernatant was collected and added to protein-G beads (Life Technologies) pre-bound with 50 μg each of anti-GFP monoclonal antibodies HtzGFP-19C8 and HtzGFP-19F7 (Monoclonal Antibody Core Facility, Sloan-Kettering Cancer Center) and incubated at 4°C for 30 min. Beads were collected and washed with Wash Buffer #2 (20 mM HEPES [pH 7.4], 300 mM KCl, 5 mM MgCl, 1% Igepal CA-360) three times. RNA was eluted from the beads by addition of 350 μl of RLT buffer (QIAGEN) and incubated for 5 min with occasional inversion. RNA is then isolated using the RNAmin elute kit from QIAGEN. RNA was then amplified in a linear fashion using Arcturus RiboAmp HS kit (Life Technologies). cDNA was then generated for quality assessment and then paired-end Illumina, multiplexed sequencing libraries were prepared.

Library Preparation from Cells Isolated by FACS

Cell dissociation procedures, FACS purification of cells from 40 and 53 hr APF, RNA purification, and library constructions were done as described in Tan et al. (2015).

Additional experimental procedures are included in the Supplemental Information.

SUPPLEMENTAL INFORMATION

Supplemental Information includes Supplemental Experimental Procedures, five figures, and eight tables and can be found with this article online at http://dx.doi.org/10.1016/j.celrep.2015.12.102.

AUTHOR CONTRIBUTIONS

K.X.Z., J.M., and S.L.Z. designed and conceived research. J.M.M. generated T-TRAP constructs and flies, performed dissections and biochemical RNA isolation, and prepared libraries. L.T. performed FACS experiments. K.X.Z. collected Illumina sequencing data, developed data analysis pipelines, and analyzed data. M.P. designed data analysis pipelines. K.X.Z., J.M.M, and S.L.Z. interpreted data and wrote the paper.

ACKNOWLEDGMENTS

We would like to thank Douglas Black, Kelsey Martin, William Yang, Kathrin Plath, Giovanni Coppola, and members of the S.L.Z. laboratory for critical reading of the manuscript. K.X.Z. is supported by the Canadian Institute of Health Research Fellowship. J.M.M. was supported by the NIH-Cellular Neurobiology Training Program (5T32NS07101:29-30). S.L.Z. is an investigator of the Howard Hughes Medical Institute.

Received: April 30, 2014
Revised: December 4, 2015
Accepted: December 21, 2015
Published: January 28, 2016

REFERENCES

Abruzzi, K., Chen, X., Nagoshi, E., Zadina, A., and Rosbash, M. (2015). RNA-seq profiling of small numbers of Drosophila neurons. Methods Enzymol. *551*, 369–386.

Bate, M. (1993). The Development of Drosophila Melanogaster. M. Bate and A. Martinez-Arias, eds. (Cold Spring Harbor Press), pp. 1363–1491.

Berkovits, B.D., and Mayr, C. (2015). Alternative 3′ UTRs act as scaffolds to regulate membrane protein localization. Nature *522*, 363–367.

Bhattacharya, S., Stewart, B.A., Niemeyer, B.A., Burgess, R.W., McCabe, B.D., Lin, P., Boulianne, G., O'Kane, C.J., and Schwarz, T.L. (2002). Members of the synaptobrevin/vesicle-associated membrane protein (VAMP) family in Drosophila are functionally interchangeable in vivo for neurotransmitter release and cell viability. Proc. Natl. Acad. Sci. USA *99*, 13867–13872.

Chen, Y., Akin, O., Nern, A., Tsui, C.Y., Pecot, M.Y., and Zipursky, S.L. (2014). Cell-type-specific labeling of synapses in vivo through synaptic tagging with recombination. Neuron *81*, 280–293.

Cheng, H.J., Nakamoto, M., Bergemann, A.D., and Flanagan, J.G. (1995). Complementary gradients in expression and binding of ELF-1 and Mek4 in development of the topographic retinotectal projection map. Cell *82*, 371–381.

Chia, P.H., Li, P., and Shen, K. (2013). Cell biology in neuroscience: cellular and molecular mechanisms underlying presynapse formation. J. Cell Biol. *203*, 11–22.

Chia, P.H., Chen, B., Li, P., Rosen, M.K., and Shen, K. (2014). Local F-actin network links synapse formation and axon branching. Cell *156*, 208–220.

Clandinin, T.R., and Zipursky, S.L. (2000). Afferent growth cone interactions control synaptic specificity in the Drosophila visual system. Neuron *28*, 427–436.

Desai, C., Garriga, G., McIntire, S.L., and Horvitz, H.R. (1988). A genetic pathway for the development of the Caenorhabditis elegans HSN motor neurons. Nature *336*, 638–646.

Di Giammartino, D.C., Nishida, K., and Manley, J.L. (2011). Mechanisms and consequences of alternative polyadenylation. Mol. Cell *43*, 853–866.

Doyle, J.P., Dougherty, J.D., Heiman, M., Schmidt, E.F., Stevens, T.R., Ma, G., Bupp, S., Shrestha, P., Shah, R.D., Doughty, M.L., et al. (2008). Application of a translational profiling approach for the comparative analysis of CNS cell types. Cell *135*, 749–762.

Fambrough, D., and Goodman, C.S. (1996). The Drosophila beaten path gene encodes a novel secreted protein that regulates defasciculation at motor axon choice points. Cell *87*, 1049–1058.

García-Alonso, L., Fetter, R.D., and Goodman, C.S. (1996). Genetic analysis of Laminin A in Drosophila: extracellular matrix containing laminin A is required for ocellar axon pathfinding. Development *122*, 2611–2621.

Golic, K.G., and Lindquist, S. (1989). The FLP recombinase of yeast catalyzes site-specific recombination in the Drosophila genome. Cell *59*, 499–509.

Guan, Z., Buhl, L.K., Quinn, W.G., and Littleton, J.T. (2011). Altered gene regulation and synaptic morphology in Drosophila learning and memory mutants. Learn. Mem. *18*, 191–206.

Guichet, A., Wucherpfennig, T., Dudu, V., Etter, S., Wilsch-Bräuniger, M., Hellwig, A., González-Gaitán, M., Huttner, W.B., and Schmidt, A.A. (2002). Essential role of endophilin A in synaptic vesicle budding at the Drosophila neuromuscular junction. EMBO J. *21*, 1661–1672.

Hadjieconomou, D., Timofeev, K., and Salecker, I. (2011). A step-by-step guide to visual circuit assembly in Drosophila. Curr. Opin. Neurobiol. *21*, 76–84.

Hansen, H.T., Rasmussen, S.H., Adolph, S.K., Plass, M., Krogh, A., Sanford, J., Nielsen, F.C., and Christiansen, J. (2015). Drosophila Imp iCLIP identifies an RNA assemblage coordinating F-actin formation. Genome Biol. *16*, 123.

Heiman, M., Schaefer, A., Gong, S., Peterson, J.D., Day, M., Ramsey, K.E., Suárez-Fariñas, M., Schwarz, C., Stephan, D.A., Surmeier, D.J., et al. (2008). A translational profiling approach for the molecular characterization of CNS cell types. Cell *135*, 738–748.

Henry, G.L., Davis, F.P., Picard, S., and Eddy, S.R. (2012). Cell type-specific genomics of Drosophila neurons. Nucleic Acids Res. *40*, 9691–9704.

Hilgers, V., Lemke, S.B., and Levine, M. (2012). ELAV mediates 3′ UTR extension in the Drosophila nervous system. Genes Dev. *26*, 2259–2264.

Hoang, B., and Chiba, A. (1998). Genetic analysis on the role of integrin during axon guidance in Drosophila. J. Neurosci. *18*, 7847–7855.

Ji, Z., Lee, J.Y., Pan, Z., Jiang, B., and Tian, B. (2009). Progressive lengthening of 3′ untranslated regions of mRNAs by alternative polyadenylation during mouse embryonic development. Proc. Natl. Acad. Sci. USA *106*, 7028–7033.

Keleman, K., Krüttner, S., Alenius, M., and Dickson, B.J. (2007). Function of the Drosophila CPEB protein Orb2 in long-term courtship memory. Nat. Neurosci. *10*, 1587–1593.

Kidd, T., Brose, K., Mitchell, K.J., Fetter, R.D., Tessier-Lavigne, M., Goodman, C.S., and Tear, G. (1998). Roundabout controls axon crossing of the CNS midline and defines a novel subfamily of evolutionarily conserved guidance receptors. Cell *92*, 205–215.

Kopczynski, C.C., Davis, G.W., and Goodman, C.S. (1996). A neural tetraspanin, encoded by late bloomer, that facilitates synapse formation. Science *271*, 1867–1870.

Kozomara, A., and Griffiths-Jones, S. (2014). miRBase: annotating high confidence microRNAs using deep sequencing data. Nucleic Acids Res. *42*, D68–D73.

Kumar, J.P., and Ready, D.F. (1995). Rhodopsin plays an essential structural role in Drosophila photoreceptor development. Development *121*, 4359–4370.

Kurusu, M., Cording, A., Taniguchi, M., Menon, K., Suzuki, E., and Zinn, K. (2008). A screen of cell-surface molecules identifies leucine-rich repeat proteins as key mediators of synaptic target selection. Neuron *59*, 972–985.

Lee, C.H., Herman, T., Clandinin, T.R., Lee, R., and Zipursky, S.L. (2001). N-cadherin regulates target specificity in the Drosophila visual system. Neuron *30*, 437–450.

Lee, R.C., Clandinin, T.R., Lee, C.H., Chen, P.L., Meinertzhagen, I.A., and Zipursky, S.L. (2003). The protocadherin Flamingo is required for axon target selection in the Drosophila visual system. Nat. Neurosci. *6*, 557–563.

Liebl, F.L., Wu, Y., Featherstone, D.E., Noordermeer, J.N., Fradkin, L., and Hing, H. (2008). Derailed regulates development of the Drosophila neuromuscular junction. Dev. Neurobiol. *68*, 152–165.

Ly, C.V., Yao, C.K., Verstreken, P., Ohyama, T., and Bellen, H.J. (2008). straightjacket is required for the synaptic stabilization of cacophony, a voltage-gated calcium channel alpha1 subunit. J. Cell Biol. *181*, 157–170.

Medioni, C., Ramialison, M., Ephrussi, A., and Besse, F. (2014). Imp promotes axonal remodeling by regulating profilin mRNA during brain development. Curr. Biol. *24*, 793–800.

Menon, K.P., Sanyal, S., Habara, Y., Sanchez, R., Wharton, R.P., Ramaswami, M., and Zinn, K. (2004). The translational repressor Pumilio regulates presynaptic morphology and controls postsynaptic accumulation of translation factor eIF-4E. Neuron *44*, 663–676.

Millard, S.S., Lu, Z., Zipursky, S.L., and Meinertzhagen, I.A. (2010). Drosophila dscam proteins regulate postsynaptic specificity at multiple-contact synapses. Neuron *67*, 761–768.

Nern, A., Pfeiffer, B.D., and Rubin, G.M. (2015). Optimized tools for multicolor stochastic labeling reveal diverse stereotyped cell arrangements in the fly visual system. Proc. Natl. Acad. Sci. USA *112*, E2967–E2976.

Newsome, T.P., Asling, B., and Dickson, B.J. (2000). Analysis of Drosophila photoreceptor axon guidance in eye-specific mosaics. Development *127*, 851–860.

Pfeiffer, B.D., Truman, J.W., and Rubin, G.M. (2012). Using translational enhancers to increase transgene expression in Drosophila. Proc. Natl. Acad. Sci. USA *109*, 6626–6631.

Ray, D., Kazan, H., Cook, K.B., Weirauch, M.T., Najafabadi, H.S., Li, X., Gueroussov, S., Albu, M., Zheng, H., Yang, A., et al. (2013). A compendium of RNA-binding motifs for decoding gene regulation. Nature *499*, 172–177.

Rivera-Alba, M., Vitaladevuni, S.N., Mishchenko, Y., Lu, Z., Takemura, S.Y., Scheffer, L., Meinertzhagen, I.A., Chklovskii, D.B., and de Polavieja, G.G. (2011). Wiring economy and volume exclusion determine neuronal placement in the Drosophila brain. Curr. Biol. *21*, 2000–2005.

Samson, M.L., and Chalvet, F. (2003). found in neurons, a third member of the Drosophila elav gene family, encodes a neuronal protein and interacts with elav. Mech. Dev. *120*, 373–383.

Schmucker, D., Clemens, J.C., Shu, H., Worby, C.A., Xiao, J., Muda, M., Dixon, J.E., and Zipursky, S.L. (2000). Drosophila Dscam is an axon guidance receptor exhibiting extraordinary molecular diversity. Cell *101*, 671–684.

Serafini, T., Kennedy, T.E., Galko, M.J., Mirzayan, C., Jessell, T.M., and Tessier-Lavigne, M. (1994). The netrins define a family of axon outgrowth-promoting proteins homologous to C. elegans UNC-6. Cell *78*, 409–424.

Smith, L.A., Wang, X., Peixoto, A.A., Neumann, E.K., Hall, L.M., and Hall, J.C. (1996). A Drosophila calcium channel alpha1 subunit gene maps to a genetic locus associated with behavioral and visual defects. J. Neurosci. *16*, 7868–7879.

Steiner, F.A., Talbert, P.B., Kasinathan, S., Deal, R.B., and Henikoff, S. (2012). Cell-type-specific nuclei purification from whole animals for genome-wide expression and chromatin profiling. Genome Res. *22*, 766–777.

Stevens, R.J., Akbergenova, Y., Jorquera, R.A., and Littleton, J.T. (2012). Abnormal synaptic vesicle biogenesis in Drosophila synaptogyrin mutants. J. Neurosci. *32*, 18054–18067.

Takemura, S.Y., Bharioke, A., Lu, Z., Nern, A., Vitaladevuni, S., Rivlin, P.K., Katz, W.T., Olbris, D.J., Plaza, S.M., Winston, P., et al. (2013). A visual motion detection circuit suggested by Drosophila connectomics. Nature *500*, 175–181.

Tan, L., Zhang, K.X., Pecot, M.Y., Nagarkar-Jaiswal, S., Lee, P.T., Takemura, S.Y., McEwen, J.M., Nern, A., Xu, S., Tadros, W., et al. (2015). Ig Superfamily ligand and receptor pairs expressed in synaptic partners in Drosophila. Cell *163*, 1756–1769.

Tuthill, J.C., Nern, A., Holtz, S.L., Rubin, G.M., and Reiser, M.B. (2013). Contributions of the 12 neuron classes in the fly lamina to motion vision. Neuron *79*, 128–140.

Van Epps, H., Dai, Y., Qi, Y., Goncharov, A., and Jin, Y. (2010). Nuclear pre-mRNA 3′-end processing regulates synapse and axon development in C. elegans. Development *137*, 2237–2250.

Venken, K.J., Simpson, J.H., and Bellen, H.J. (2011). Genetic manipulation of genes and cells in the nervous system of the fruit fly. Neuron *72*, 202–230.

Vilinsky, I., Stewart, B.A., Drummond, J., Robinson, I., and Deitcher, D.L. (2002). A Drosophila SNAP-25 null mutant reveals context-dependent redundancy with SNAP-24 in neurotransmission. Genetics *162*, 259–271.

Wan, H.I., DiAntonio, A., Fetter, R.D., Bergstrom, K., Strauss, R., and Goodman, C.S. (2000). Highwire regulates synaptic growth in Drosophila. Neuron *26*, 313–329.

Yamagata, M., and Sanes, J.R. (2008). Dscam and Sidekick proteins direct lamina-specific synaptic connections in vertebrate retina. Nature *451*, 465–469.

Zaharieva, E., Haussmann, I.U., Bräuer, U., and Soller, M. (2015). Concentration and localization of coexpressed ELAV/Hu proteins control specificity of mRNA processing. Mol. Cell. Biol. *35*, 3104–3115.

Zallen, J.A., Kirch, S.A., and Bargmann, C.I. (1999). Genes required for axon pathfinding and extension in the C. elegans nerve ring. Development *126*, 3679–3692.

Zhu, B., Pennack, J.A., McQuilton, P., Forero, M.G., Mizuguchi, K., Sutcliffe, B., Gu, C.J., Fenton, J.C., and Hidalgo, A. (2008). Drosophila neurotrophins reveal a common mechanism for nervous system formation. PLoS Biol. *6*, e284.

Zlatic, M., Li, F., Strigini, M., Grueber, W., and Bate, M. (2009). Positional cues in the Drosophila nerve cord: semaphorins pattern the dorso-ventral axis. PLoS Biol. *7*, e1000135.